Control Design for Balancing a Motorbike at Zero Longitudinal Speed

Hanna Zsofia Horvath[1], Denes Takacs[2]
[1] Department of Applied Mechanics, Budapest University of Technology and Economics,
[2] MTA-BME Research Group on Dynamics of Machines and Vehicles
E-mail: hanna.horvath@mm.bme.hu

Vehicle stability is a critical factor while riding a motorcycle. Due to the complexity of the spatial mechanical model and the related governing equations, the investigations are limited to linear stability analysis. The equations of motion are derived analytically with the help of Kane's method. A control algorithm is designed in order to stabilize the motorcycle at zero longitudinal speed using the steering mechanism. The linear stability properties are analyzed numerically, namely, we use semi-discretization and the Multidimensional Bisection Method to construct the stability charts of the delayed feedback controller. The optimal control gains are selected. The stable and unstable oscillations of the lean and the steering angles are plotted as a result of numerical simulations. It is shown that with a negative trail the stable domain of the control gains is larger and the vibrations decay faster.

Topics / Modeling, Vehicle Dynamics Theory

1. INTRODUCTION

The investigation of the balancing motorbike is a complex task, since no in-plane models can appropriately describe the dynamics of such vehicles. Moreover, the complex structure of the geometric and kinematic constraints of the spatial mechanical model provides a set of nonlinear differential equations that cannot be managed analytically. Therefore, semi-analytical and numerical analyses are generally used in the literature to analyze the dynamics of the motorbike [1-5], and mainly the validity of these studies are limited to small vibrations. In this study, we also focus on the linear stability of the motorbike. Based on the idea of Honda Riding Assist [6], we examine the case when the motorbike is balanced by its steering mechanism at zero longitudinal speed.

We use a spatial mechanical model that is based on the Whipple bicycle model [7], [8]. The governing equations are derived with the help of Kane's method [9]. The linear stability properties are analyzed; the linear stability charts are constructed by semi-discretization [10] and with the help of the Multidimensional Bisection Method [11]. The effects of several geometric parameters and the feedback delay in the control law are shown. The optimal control gains, for which the characteristic multiplier is the smallest, are selected. The stability properties are checked by means of numerical simulations.

2. MECHANICAL MODEL AND GOVERNING EQUATIONS

We use the mechanical model shown in panel (a) of Fig. 1. This bicycle model, which has also been studied by Meijaard et al. [8] as a benchmark model, consists of four rigid bodies: the front and the rear wheels, the fork and the frame. The parameters that are in the focus of our study, namely the trail e and the rake angle ε, are depicted in panel (b) of Fig. 1.

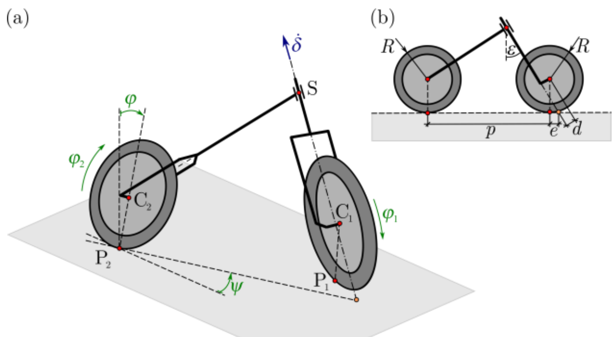

Fig. 1 Spatial mechanical model of the motorcycle (a) and the side view for $\psi = 0, \varphi = 0$ and $\delta = 0$ with the relevant geometric parameters (b)

All four bodies have six degrees of freedom (DoF) without constraints, leading to 24 DoF altogether. Each of the three hinges between the bodies constraint three translational and two rotational DoFs. The front and the rear wheels are attached to the ground leading to two additional geometric constraints. Therefore, the vector of generalized coordinates consists of $4 \cdot 6 - 3 \cdot 5 - 2 \cdot 1 = 7$ elements and can be composed as

$$\mathbf{q} = [X\ Y\ \psi\ \varphi\ \delta\ \varphi_1\ \varphi_2]^{\mathrm{T}}, \tag{1}$$

where X and Y are the coordinates of the center point C_2 of the rear wheel, ψ is the yaw angle, φ is the lean angle of the frame, δ is the steering angle, φ_1 and φ_2 are the rotational angles of the front and the rear wheels, respectively.

Four scalar kinematic constraining equations can be formulated for the two wheels rolling on the ground plane (one longitudinal and one lateral for each wheels). Since our goal is to stabilize the motorcycle for zero longitudinal speed ($v = 0$), the rotational speed of the rear wheel is considered to be constant: $\dot{\varphi}_2 = v/R = 0$, where R is the radius of the wheels. In all, we have five kinematic constraints. The equations of motion are formulated with the help of Kane's method [9] in which we define $7 - 5 = 2$ pseudovelocities, summed up in a vector as

$$\boldsymbol{\sigma} = [\dot{\varphi}\ \dot{\delta}]^{\mathrm{T}}. \qquad (2)$$

Since the nonlinear equations of motion do not have a compact formulation, we strict ourselves to the linearized equations. By collecting the constant coefficients for the lean and steering angles from the Kane's equations and considering zero longitudinal speed, namely $v = 0$, the linearized equations of motion can be written as

$$\mathbf{M}\ddot{\mathbf{x}} + g\mathbf{K}_0\mathbf{x} = \mathbf{f}, \qquad (3)$$

where $\mathbf{x} = [\varphi\ \delta]^{\mathrm{T}}$ and $\mathbf{f} = [0\ M]^{\mathrm{T}}$ with the internal steering torque M. In Eq. (3), $\mathbf{M}$ is the mass matrix, $\mathbf{K}_0$ is the velocity-independent stiffness matrix and g is the gravitational acceleration. The above described linearized equations of motion agree with the study of Meijaard et al. [8].

3. CONTROL DESIGN

Our goal is to stabilize the motorcycle using the steering mechanism. As a first step, we use a simple PD controller with feedback delay τ. A higher level controller calculates the desired steering angle as

$$\delta_{\mathrm{des}} = -K_{\mathrm{p}\varphi}\varphi(t-\tau) - K_{\mathrm{d}\varphi}\,\dot{\varphi}(t-\tau), \qquad (4)$$

where $K_{\mathrm{p}\varphi}$ and $K_{\mathrm{d}\varphi}$ are proportional and derivative gains for the lean angle. The internal steering torque M is created by a lower level control as

$$M = -K_{\mathrm{p}\delta}(\delta(t) - \delta_{\mathrm{des}}) - K_{\mathrm{d}\delta}\,\dot{\delta}(t), \qquad (5)$$

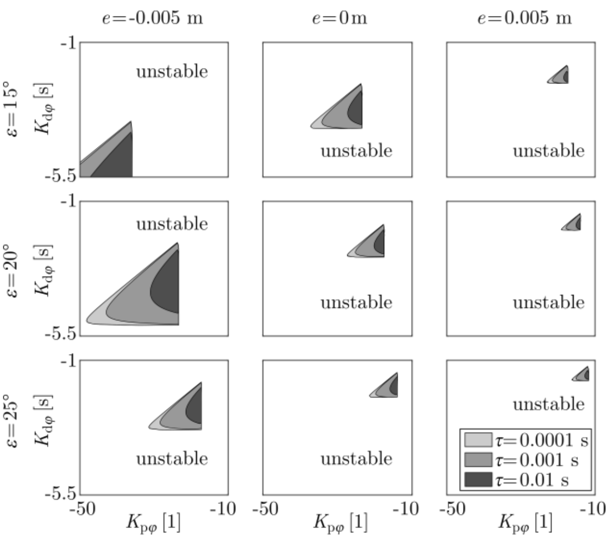

Fig. 2 Linear stability charts considering different parameter values for the trail e, the rake angle ε and the feedback delay τ

where $K_{\mathrm{p}\delta}$ and $K_{\mathrm{d}\delta}$ are the proportional and derivative gains for the steering angle.

Linear stability charts are drawn in the $K_{\mathrm{p}\varphi} - K_{\mathrm{d}\varphi}$ plane considering different parameter values for the trail e, the rake angle ε and the feedback delay τ, see Fig. 2. Other geometric parameters were fixed and chosen based on a small-scale experimental model of [12]. The control gains for the steering angle were fixed as $K_{\mathrm{p}\delta} = 100$ Nm and $K_{\mathrm{d}\delta} = 10$ Nms.

The stability boundaries were determined with the help of semi-discretization [10]. In the linear stability charts, the linearly stable domains are shaded with different intensity corresponding to the value of the feedback delay.

As it can be seen in the panels of Fig. 2, by increasing the rake angle ε, the linearly stable region is shifted and shrunken. The greater the feedback delay τ is, the smaller the linearly stable domain is. Most importantly, the effect of the trail e can also be seen. It can be observed, that having a negative trail increases the stable domain. Namely, in contrast to the requirements of the high speed stability of the motorcycle, the negative trail is beneficial for the balancing task. This agrees with the concept of Honda Riding Assist [6], where they use a special mechanism at the front fork of the motorcycle to modify the trail for the balancing task.

For fixed feedback delay $\tau = 0.01$ s and different parameter values for the trail e and the rake angle ε, the optimal points were chosen, for which the absolute value of the characteristic multiplier is the smallest. The corresponding control gains and the characteristic multipliers are summarized in Table 1. As can be seen, the characteristic multipliers only differ in the fourth digit. However, larger control gains are needed for the same rake angle but a negative trail, which can also be seen in the linear stability charts of Fig. 2.

Table 1 The control gains and the characteristic multipliers for the optimal points in case of feedback delay $\tau = 0.01$ s

e [m]	ε [°]	$K_{\mathrm{p}\varphi}{}^{\mathrm{opt}}$ [1]	$K_{\mathrm{d}\varphi}{}^{\mathrm{opt}}$ [s]	Multipl. [1]
-0.005	15	-41.507	-6.1807	0.998289
0	15	-24.294	-3.0496	0.998047
0.005	15	-17.528	-2.0721	0.997919
-0.005	20	-25.656	-3.5315	0.998198
0	20	-18.168	-2.2703	0.998084
0.005	20	-14.284	-1.7117	0.998071
-0.005	25	-18.368	-2.4099	0.998177
0	25	-14.404	-1.7793	0.998113
0.005	25	-11.962	-1.4324	0.998094

The optimal points are marked in the stability chart of Fig. 3 for trail $e = -0.005$ m and rake angle $\varepsilon = 25°$. For decreasing feedback delay values, the optimal point goes near the stability boundary. On the one hand, this may be against our physical sense. On the other hand, the characteristic multipliers are nearly the same in a large part of the stable domain, so the location of the optimal point is not significant.

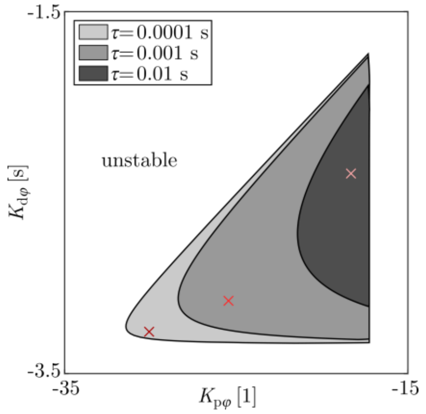

Fig. 3 The linear stability charts and the optimal points for $e = -0.005$ m, $\varepsilon = 25°$ and for different values of the feedback delay τ

4. NUMERICAL SIMULATIONS

The stability properties are verified with numerical simulations, for which the governing equations are rewritten in first order form:

$$\dot{\mathbf{y}}(t) = \mathbf{A}\,\mathbf{y}(t) + \mathbf{B}\,\mathbf{y}(t-\tau)\,, \tag{6}$$

where $\mathbf{y}(t) = [\varphi\ \delta\ \dot{\varphi}\ \dot{\delta}]^{\mathrm{T}}$ is the vector of the state variables, $\mathbf{A}$ and $\mathbf{B}$ correspond to the coefficient matrices of the non-delayed and the delayed terms, respectively. The *DDE23 Matlab* routine was used with initial condition $\mathbf{y}(t) = [\varphi\ \delta\ \dot{\varphi}\ \dot{\delta}]^{\mathrm{T}} = \mathbf{0}$ for $t \in [-\tau, 0)$ and $\mathbf{y}(0) = [0\ 0\ \dot{\varphi}_0\ 0]^{\mathrm{T}}$, where $\dot{\varphi}_0 = \dot{\varphi}(0)$ was an impact-like perturbation.

In Fig. 4, the stability boundaries in the plane of the control gains are plotted with semi-discretization [10] and with the help of the Multidimensional Bisection Method [11] for trail $e = -0.005$ m, rake angle $\varepsilon = 25°$ and feedback delay $\tau = 0.01$ s. The linearly stable domain is shaded in dark gray. A static stability boundary ($\omega = 0$) can be observed approximately at $K_{p\varphi} = -17.2$, see the vertical line. The parameter points for which numerical simulations are run, are also depicted in Fig. 4 and the corresponding control gains and the values of the initial perturbation are summarized in Table 2.

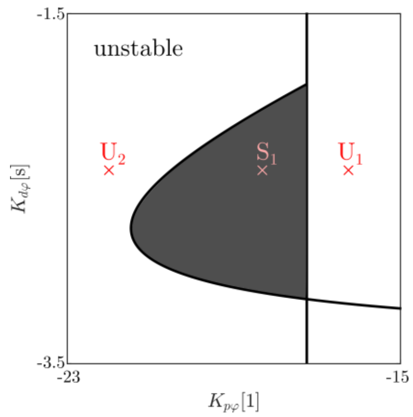

Fig. 4 The stability boundaries in the plane of the control gains for $e = -0.005$ m, $\varepsilon = 25°$ and $\tau = 0.01$ s

Table 2 The control gains for the parameter points depicted in Fig. 4 and the initial perturbation used in the numerical simulations

point	${K_{p\varphi}}^{opt}$ [1]	${K_{d\varphi}}^{opt}$ [s]	$\dot{\varphi}_0$ $\left[\frac{rad}{s}\right]$
S_1	-18.368	-2.4099	0.01
U_1	-16.250	-2.4099	0.001
U_2	-22.000	-2.4099	0.001

The time histories of the lean angle φ and the steering angle δ can be seen in Fig. 5, 6 and 7 for trail $e = -0.005$ m, rake angle $\varepsilon = 25°$ and feedback delay $\tau = 0.01$ s. For the optimal point S_1, the vibrations decay rapidly, see Fig. 5.

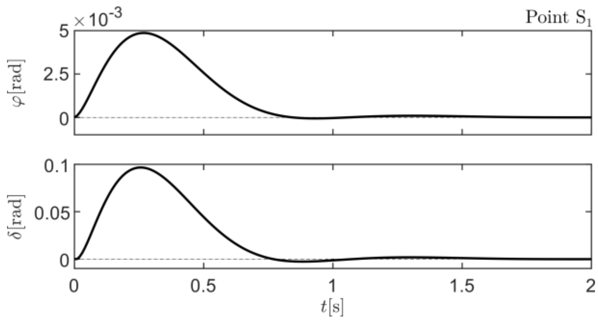

Fig. 5 The time histories of the lean angle φ and the steering angle δ for point S_1 (optimal point)

For point U_1, static loss of stability can be observed, i.e., the motorcycle loses its stability without oscillations, see Fig. 6. This means that a single real characteristic multiplier leaves the unit circle. As can be seen in Fig. 7, the motorcycle loses its stability via oscillations, that is, dynamics loss of stability occurs for point U_2. This corresponds to the pair of complex-conjugate characteristic multipliers leaving the unit circle.

The time histories are also plotted for fixed rake angle and feedback delay values, but different parameter

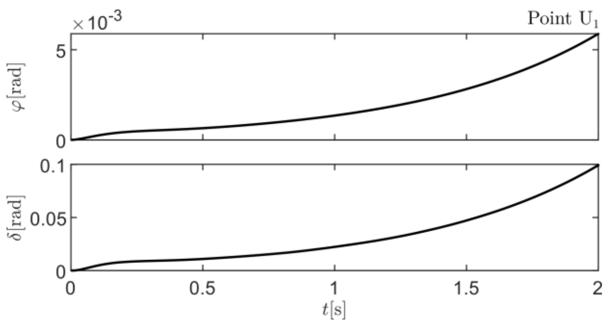

Fig. 6 The time histories of the lean angle φ and the steering angle δ for point U_1 (static loss of stability)

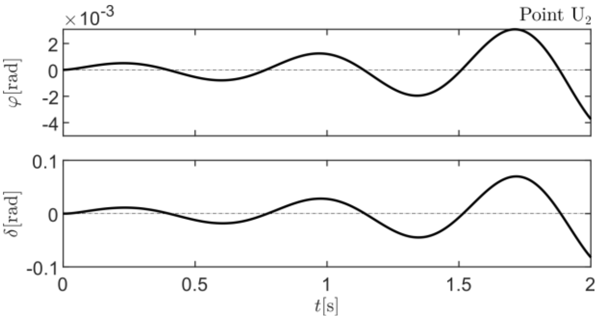

Fig. 7 The time histories of the lean angle φ and the steering angle δ for point U_2 (dynamic loss of stability)

values of the trail e, see Fig. 8. The initial perturbation was $\dot{\varphi}_0 = 0.0075$ rad/s. As can be seen, the vibrations decay faster for negative trail (see the black curves) than for zero or positive trail (see the blue and the red curves, respectively). Therefore, numerical simulations also confirm that having a negative trail is beneficial for the balancing task at zero longitudinal speed.

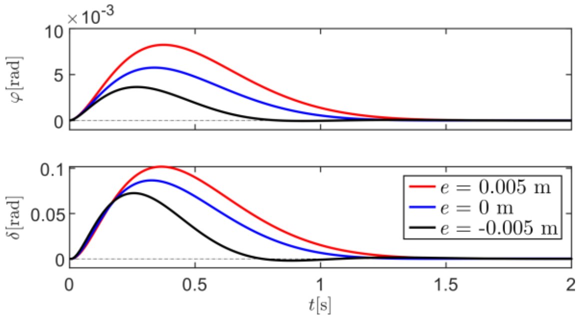

Fig. 7 The time histories of the lean angle φ and the steering angle δ for different parameter values of the trail e, when $\varepsilon = 25°$ and $\tau = 0.01$ s

5. CONCLUSIONS

The spatial mechanical model and the linearized equations of motion are used to investigate the balancing of the motorcycle at zero longitudinal speed. A hierarchical linear feedback controller was constructed with feedback delay. The linear stability charts were drawn for some geometric parameter values and the feedback delay. The time histories for the lean and the steering angles were also shown for some control gain pairs. Examples of static and dynamic loss of stability were presented.

It was shown, that with a positive trail, the stable domain is narrow and the feedback delay has to be small in order to balance the motorcycle successfully. It was confirmed by the numerical simulations that the vibrations decay faster when the trail is negative.

The experimental validation of the theoretical results is a future task, as like as the nonlinear analysis of the motorcycle balancing task.

ACKNOWLEDGEMENTS

This research was partly supported by the János Bolyai Research Scholarship of the Hungarian Academy of Sciences and by the National Research, Development and Innovation Office under Grant No. NKFI-128422.

Supported by the ÚNKP-21-3 New National Excellence Program of the Ministry for Innovation and Technology from the source of the National Research, Development and Innovation Fund.

REFERENCES

[1] Sharp, R. S. et al. "Advances in the modelling of motorcycle dynamics", Multibody Syst. Dyn. 12(3), 2004, pp. 251–283.

[2] Kooijman, J. D. G. et al. „Experimental validation of a model of an uncontrolled bicycle", Multibody Syst. Dyn. 19, 2008, pp. 115–132. https://doi.org/10.1007/s11044-007-9050-x

[3] Plöchl, M. et al. "On the wobble mode of a bicycle", Vehic. Syst. Dyn. 50(3), 2012, pp. 415–429. https://doi.org/10.1080/00423114.2011.594164

[4] Klinger, F. et al. "Wobble of a racing bicycle with a rider hands on and hands off the handlebar", Vehic. Syst. Dyn. 52, 2014, pp. 51–68. https://doi.org/10.1007/978-3-322-89521-9_13

[5] Edelmann, J. et al. "Bicycle rider control modelling for path tracking", IFAC-PapersOnLine 48 (1), 2015, pp. 55–60. https://doi.org/10.1016/j.ifacol.2015.05.070

[6] Honda Motor Company Ltd. Honda Riding Assist. https://global.honda/innovation/CES/2017/002.html.

[7] Whipple, F. J. W. "The Stability of the Motion of a Bicycle", Quart. J. Pure Appl. Math., 1899, pp. 312-348.

[8] Meijaard, J. P. et al. "Linearized Dynamics Equations for the Balance and Steer of a Bicycle: A Benchmark and Review", Proc. of Royal Society A, 2007, pp. 1955–1982.

[9] Kane, T. R. et al. "Dynamics: Theory and Applications", McGraw-Hill Book Company, 1985.

[10] Insperger, T. et al. "Semi-discretization", Springer NY, 2011, pp. 39-71.

[11] Bachrathy, D., and Stepan, G. "Bisection method in higher dimensions and the efficiency number". Periodica Polytechnica - Mechanical Engineering, 56(2), 2012, pp. 81–86.

[12] Szabó, A. et al. "Simplified mechanical model for balancing a motorbike with steering at zero speed", ECCOMAS Thematic Conference on Multibody Dynamics, 2021.